大橋暁，大西五三男，別所雅彦，松本卓也，松山順太郎，中村耕三	CT・CAD/有限要素法解析を用いた創外固定ピン応力の検討 非対称ピンプロファイルはピンと骨の界面における応力集中を軽減する	骨折	29(Suppl.)	S193	2007
別所雅彦，大西五三男，松本卓也，大橋暁，飛田健治，中村耕三	CT/有限要素法による骨強度評価 薬剤投与による大腿骨近位部の強度の変化について	骨折	29(Suppl.)	S71	2007
松本卓也，大西五三男，別所雅彦，大橋暁，飛田健治，中村耕三	CT/有限要素法による大腿骨外傷後骨欠損例の骨強度評価	骨折	29(Suppl.)	S42	2007
大橋暁，大西五三男，別所雅彦，松本卓也，松山順太郎，中村耕三	CT・CAD/有限要素解析を用いた創外固定ピン骨インターフェース応力分布の検討	日本整形外科学会雑誌	81(3)	S209	2007
松山順太郎，大西五三男，別所雅彦，大橋暁，松本卓也，中村耕三，酒井亮一，鈴木浩之，大塚利樹，宮坂好一，原田烈光	超音波エコートラッキング法を用いた骨癒合判定法	日本創外固定・骨延長学会雑誌	18	127	2007
大橋 暁、大西 五三男、別所 雅彦、松本 卓也、松山順太郎、中村 耕三第	CT・CAD/有限要素法解析を用いた創外固定ピン応力の検討一非対称ピンプロファイルはピンと骨の界面における応力集中を軽減する一、	日本創外固定・骨延長学会雑誌	19	71	2007
別所雅彦、大西五三男、松本卓也、大橋 暁、飛田健治、中村耕三	CT 画像を用いた有限要素法非線形解析による大腿骨近位部の骨強度評価 —荷重・拘束条件の相違による予測骨強度の相違について—	Osteoporosis Japan	15(Suppl. 1)	156	2007
松本卓也、大西五三男、別所雅彦、大橋 暁、飛田健治、中村耕三	CT/有限要素法による脊椎椎体の強度解析 —日常生活における骨強度評価への応用—	Osteoporosis Japan	15(Suppl. 1)	156	2007
別所雅彦、大西五三男、松本卓也、大橋暁、飛田健治、中村耕三	新鮮死体大腿骨標本のCT 有限要素法による予測骨折荷重の正確性の検証	日本コンピュータ外科学会誌	9 (3)	99-100	2007
松本卓也、大西五三男、別所雅彦、大橋暁、飛田健治、中村耕三	CT/有限要素法による骨強度評価の臨床応用	日本コンピュータ外科学会誌	9(3)	107-8	2007
Imai K, Ohnishi I, Yamamoto S, Nakamura K.	In vivo assessment of lumbar vertebral strength in elderly women using computed tomography-based nonlinear finite element model.	Spine	33 (1)	27-32	2008

Bessho, Masahiko; Ohnishi, Isao; Matsumoto, Takuya; Ohashi, Satoru; Tobita, Kenji; Matsuyama, Juntaro; Nakamura, Kozo	Prediction of strength and fracture location of the proximal femur by a CT-based nonlinear finite element method - Effect of load direction on hip fracture load and fracture site -	Transactions of orthopaedic research society	33	955	2008
Ohashi, Satoru; Ohnishi, Isao; Matsuyama, Juntaro; Bessho, Masahiko; Matsumoto, Takuya; Nakamura, Kozo	An Asymmetrical Thread Profile External Fixation Pin has Higher Pullout Strength than a Symmetrical Thread Pin	Transactions of orthopaedic research society	33	1050	2008
松本卓也，飛田健治，大西五三男，大橋暁，別所雅彦，中村耕三	3次元CT画像とCADデータを用いた手術シュミレーションの試み	日本創外固定・骨延長学会雑誌	20	105	2008
飛田健治、大西五三男、別所雅彦、松本卓也 大橋暁、中村耕三	3次元CT画像を基にした管骨変形評価法 Deformity Evaluation of the Tubular Bone Using 3D CT Image	日本創外固定・骨延長学会雑誌	20	61	2008
大橋 暁、大西 五三男、別所 雅彦、松本 卓也、松山 順太郎、中村 耕三	Universal-Bar-Link 創外固定器を用いた変形矯正における固定器設置位置・角度の誤差許容範囲の検討	日本創外固定・骨延長学会雑誌	20	104	2008
Matsuyama J, Ohnishi I, Sakai R, Bessho M, Matsumoto T, Miyasaka K, Harada A, Ohashi S, Nakamura K.	A New Method for Evaluation of Fracture Healing by Echo Tracking.	Ultrasound Medicine & Biol	In press		
鄭常賢、加門大和、廖洪恩、光石衛、中島義和、小山毅、菅野伸彦、前田ゆき、別所雅彦、大橋暁、松本卓也、岩城純一郎、中沢東治、大西五三男、中村耕三、佐久間一郎	直達式骨折整復を支援する骨折整復システムの開発、	先端医療開発研究シンポジウム講演抄録集		pp51	2008
鄭常賢、廖洪恩、小林英津子、光石衛、中島義和、小山毅、菅野伸彦、前田ゆき、別所雅彦、大橋暁、松本卓也、大西五三男、佐久間一郎	直達式骨折整復の臨床データ取得システム	第16回日本コンピュータ外科学会大会 第17回コンピュータ支援画像診断学会大会 合同論文集		pp59-60	2007

Nakajima Y, Tashiro T, Sugano N, Yonenobu K, Koyama T, Maeda Y, Tamura Y, Saito M, Tamura S, Mitsuishi M, Sugita N, Sakuma I, Ochi T, Matsumoto Y.	Fluoroscopic bone fragment tracking for surgical navigation in femur fracture reduction by incorporating optical tracking of hip joint rotation center.	IEEE Transactions on Biomedical Engineering	54(9)	1703-1706	2007
Okada T, Iwasaki Y, Koyama T, Sugano N, Chen Y-W, Yonenobu K, Sato Y.	Computer-assisted preoperative planning for reduction of proximal femoral fracture using 3D-CT data.	IEEE Transactions on Biomedical Engineering	55	印刷中	2008
Maeda Y, Sugano N, Saito M, Yonenobu K, Sakuma I, Nakajima Y, Warisawa S, Mitsuishi M	Robot-assisted femoral fracture reduction. Preliminary study in patients and healthy volunteers.	Computer Aided Surgery	13	印刷中	2008
Y. Cheng, S. Wang, T. Yamazaki, J. Zhao, Y. Nakajima, S. Tamura	Hip cartilage thickness measurement accuracy improvement	Computerized Medical Imaging and Graphics	Vol.31,no.8	643-655	2007

Ⅲ　研究成果の刊行物・印刷

05(XII)-55

脚の牽引回旋に対する力・トルク計測
—大腿骨骨折整復ロボティック手術における脚荷重からの骨位置姿勢推定にむけて—

森 泰元[a], 中島義和[a], 杉田直彦[a], 割澤伸一[a], 光石 衛[a], 前田ゆき[e], 菅野伸彦[f], 斉藤正伸[e], 米延策雄[e], 佐久間一郎[b], 土肥健純[c], 大西五三男[d], 中村耕三[d]
東京大学大学院{[a]工学系研究科, [b]新領域創成科学研究科, [c]情報理工学系研究科, [d]医学系研究科}, [e]大阪南医療センター, [f]大阪大学大学院医学系研究科

Force and Torque Measurement in Leg Traction and Rotation
-Toward Bone Position Estimation from Leg Load in Robotic Surgery of Femur Fracture Reduction-

Y. Mori[a], Y. Nakajima[a], N. Sugita[a], S. Warisawa[a], M. Mitsuishi[a], Y. Maeda[e], N. Sugano[f], M. Saito[e], K. Yonenobu[e], I. Sakuma[b], T. Dohi[c], I. Ohnishi[d], K. Nakamura[d]
{[a]*Graduate School of Engineering*, [b]*Graduate School of Frontier Sciences*, [c]*Graduate School of Information Science and Technology*, [d]*Graduate School of Medicine*},*the University of Tokyo*, [e]*National Organization Osaka Minami Medical Center*, [f]*Graduate School of Medicine,Osaka University*

Abstract: We have developed a robotic system for femur fracture reduction. Since the reduction is an operation which applies the load to a human leg containing joints, it is difficult to estimate the affected femur position and orientation in the operation. It is expected to estimate the femur position and orientation using the data from the force sensor on the robot. We used the data of the leg traction and rotation experiments on healthy subjects to examine the feasibility to build the standard model of the relationship between the load on the leg and its motion.

Key words: Robotic surgery, Femur fracture reduction, Position estimation, Leg load

1 研究の背景

大腿骨骨折，中でも特に頸部骨折は，骨粗鬆症を有する高齢者に多く，寝たきりの原因になるなど高齢化社会を迎えるにあったって大きな社会的な問題となっている．大腿骨の骨折整復手術は脚に牽引・回旋を加え，骨折箇所を整復する手術である．この作業には大きな力を必要とし，医師への体力的負担が大きい．また，より正確な整復が骨折の早期回復と再発防止につながる．ロボットによる手術支援システムの導入は，医師の負担軽減及び手術の高精度化を促す可能性を持っている．

2 従来の研究

2.1 大腿骨骨折整復手術支援システム

我々は現在，医師の負担の低減と正確な手術の実現を目的とした大腿骨骨折整復手術支援システムの開発を行っている[1]．Fig. 1 に示すように，本システムは整復手術の計画を行う手術支援ナビゲーションシステムと，実際の整復作業や医師の作業の力補助を行う骨折整復ロボットで構成する．

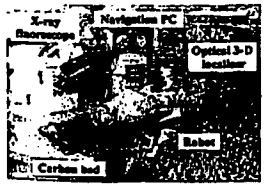

Fig. 1 Appearance of the system

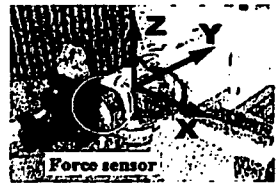

Fig. 2 Drive axes of the robot and force sensor

骨折整復ロボットは Fig. 2 に示す3軸の並進方向とそれらの周りの回転方向，計6軸の駆動軸を持つ．また，力センサを備えることで，脚に加わる荷重を3軸の力と3軸のトルクで計測する．

2.2 現在のシステムにおける問題点

大腿骨骨折の整復手術作業は，関節物体である脚に力を加える作業である(Fig. 3)．

Fig. 3 Femur fracture reduction by robot

そのため，非剛体運動をする大腿骨患部の制御が困難であり，実際の患部の位置姿勢が予定した本来の整復軌道を外れてしまった際に，ロボットが脚に過度の力を加えてしまう可能性がある．また，現在のシステムでは，実際の患部状態を随時X線撮影で確認し修正を加えながら整復を行うが，その繰り返しにより X 線被曝量が増え，手術時間も延長される．三次元位置センサを用いて大腿骨の位置姿勢を計測する方法もあるが，センサを大腿骨に直接設置するため，侵襲の大きさが問題となる．

3 大腿骨位置姿勢の予測・制御

本研究では，骨折整復ロボットで得られる情報から，骨折患部のある大腿骨の位置姿勢を予測し，制御することを目的とする．それにより，患者にとってより安全で正確な整復手術の実現と，X 線被曝の低減，手術時間の短縮を目指す．

大腿骨の位置姿勢の予測に利用できる情報は，ロボットに固定された足首の位置姿勢と，足首にかかる力・トルクの力センサによる計測値である．脛骨の位置姿勢は，足首で固定されているロボットの情報から得られるため，膝関節骨(大腿骨と脛骨)の相対位置姿勢がわかれば大腿骨の位置姿勢が求められる．ここで，脚にかかる力・トルクと膝関節骨の相対位置姿勢との関係がある関数で記述可能であると仮定する．すると，力センサの計測値から膝関節骨の相対位置姿勢，さらには大腿骨の位置姿勢が予測できる．膝関節にかかる力・トルクと膝関節骨の相対位置姿勢の関係は，大腿骨の骨折の有無に関わらない．そのため，検討に必要なデータは健常者を対象とした実験から得る．

4　実験による基礎検討

4.1　健常者下肢牽引回旋実験

脚に加えられた力・トルクと，膝関節骨の相対位置姿勢との関係を検討した．検討には大阪南医療センターにおいて計測した健常者20人の下肢牽引回旋実験のデータを用いた．この実験では，骨折整復ロボットによって被験者の脚に牽引と回旋(内旋及び外旋)をそれぞれ与え，その時の力センサの計測値を記録した．そして，得られたデータを基に，下肢の関節系の変形と脚に加えられた力・トルクとの間の関係が関数で記述できるかを検討するために，複数の被験者のデータの正規化を行った．

4.2　実験結果

4.2.1　脚の牽引に対する力・トルク

Y軸方向の牽引に対するX，Y，Zの3軸の力センサの計測値のグラフをFig. 4に示す．データは，脚にかかる重力を除去するため，ロボットが脚を把持したはじめの状態の値をゼロとした．(a)と(b)は同一被験者の左右の脚の比較を，(c)は他の被験者との比較を行ったものである．

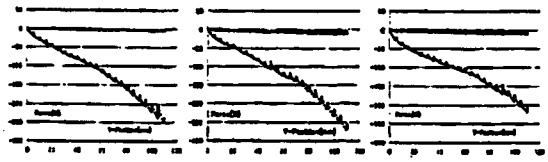

(a)Subject A, L. leg　(b)Subject A, R. leg　(c)Subject B, L. leg

Fig. 4 Traction and force

牽引方向のY軸のみに大きな力の値の変化が見られ，他の2軸の力やトルクについては大きな値は見られなかった．

次に，Y軸方向の力のデータに対して直線のあてはめを行った．Fig. 4の被験者Aのように多くの被験者のデータは，途中で折れ曲がり，傾きが変化する直線をあてはめることができ，あてはめられた直線は左右両脚でほぼ等しい傾きを持った．

4.2.2　脚の回旋に対する力・トルク

脚の回旋に対する，3軸のトルクの力センサによる計測値の原データを3次元座標上の点で表したものをFig. 5に示す．

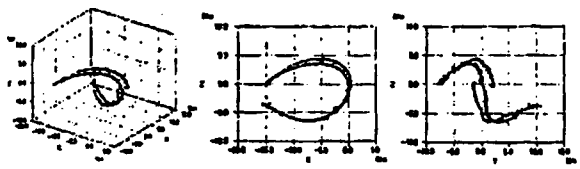

(a) Perspective view　(b)X-Z view　(c)Y-Z view

Fig. 5 Rotation and torque

原データはらせん状の曲線を描く．このデータには，脚にかかる重力によるトルクの変化の影響が含まれる．脚にかかる重力の影響は，Fig. 6に示すようにデータ上に円柱状に現れる．

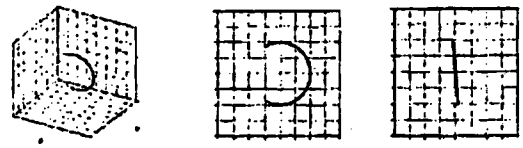

(a) Perspective view　(b)X-Z view　(c)Y-Z view

Fig. 6 Torque caused by leg weight

データ点群に対してFig. 6のような円柱をあてはめることを試みた．円柱のような形状は自動によるあてはめが困難である[2]ため，今回は手動で行った．

回旋によって脚にかかるトルクは円柱からの差分として表される．結果を見ると，脚にかかるトルクは回旋角度の増加とともに大きくなっており，重力による影響を除いた後も，回旋方向以外の軸にトルクの変化が見られた．トルクの変化は，多少の個人差は見られたものの，概ね同様の傾向を示した．

力の値についても，脚にかかる重力の方向が回旋によって変化することによる計測値の変化が見られた．しかし，重力の影響を除いた後の力の値には，大きな変化は見られなかった．

5　まとめ

健常者の下肢牽引回旋実験において，計測データから，脚にかかる重力の影響を除去し，牽引及び回旋に対して脚にかかる力とトルクを調べた．結果では，牽引量や回旋角度に対して，脚の左右や個人によらない同様の傾向が見られた．それにより，脚に加えられた荷重と脚の位置姿勢との関係を，正規化された標準モデルや関数で記述できる可能性を確認した．

今後は，脚にかかる重力の影響を自動で除去する手段を検討する．加えて，大腿骨の位置姿勢の計測など条件を見直した実験を行い，その結果を元に脚に加えられた荷重と大腿骨の位置姿勢の間の関係の，具体的な標準モデルの作成を目指す．

文献

1) Y. Nakajima, *et al.*: "Computer-assisted fracture reduction of proximal femur using preoperative CT data and intraoperative fluoroscopic images", CARS 2004, Chicago, USA (2004-06)

2) 山本正信: ユビキタスモーションキャプチャとその応用，学術講演会-人をなぞる視覚情報研究-, Osaka, Japan (2004-12)

Development of the Needle Insertion Robot for Percutaneous Vertebroplasty

S. Onogi[1], K. Morimoto[1], I. Sakuma[1], Y. Nakajima[2], T. Koyama[3], N. Sugano[3], Y. Tamura[4], S. Yonenobu[4], and Y. Momoi[5]

[1] Graduate School of Frontier Sciences, The University of Tokyo, Japan
[2] Intelligent Modeling Laboratory, the Univeristy of Tokyo, Japan
[3] Graduate School of Medicine, Osaka University, Japan
[4] Osaka Minami Medical Center, Japan
[5] Hitachi Ltd

Abstract. Percutaneous Vertebroplasty (PVP) is an effective and less invasive medical treatment for vertebral osteoporotic compression fractures. However, this operative procedure is quite difficult because an arcus vertebra, which is narrow, is needled with accuracy, and an operator's hand is exposed to X-ray continuously. We have developed a needle insertion robot for Percutaneous Vertebroplasty. Its experimental evaluation on the basic performance of the system and needle insertion accuracy are presented. A needle insertion robot is developed for PVP. This robot can puncture with accuracy and an operator does not need to be exposed to X-ray. The mechanism of the robot is compact in size (350 mm × D 400 mm × H270 mm, weight: 15 kg) so that the robot system can be inserted in the space between C-arm and the patient on the operating table. The robot system is controlled by the surgical navigation system where the appropriate needle trajectory is planned based on pre-operative three-dimensional CT images. The needle holding part of the robot is X-ray lucent so that the needle insertion process can be monitored by fluoroscopy. The position of the needle during insertion process can be continuously monitored. In vitro evaluation of the system showed that average position and orientation errors were less than 1.0 mm and 1.0 degree respectively. Experimental results showed that the safety mechanism called mechanical fuse released the needle holding disk properly when excessive force was applied to the needle. These experimental results demonstrated that the developed system has the satisfactory basic performance as needle insertion robot for PVP.

1 Introduction

Percutaneous Vertebroplasty(PVP) is an effective treatment for vertebral osteoporotic compression fractures (Figure 1). In this technique, the surgeon inserts one or two bone biopsy needles into fractured vertebral body, and injects semiliquid plastic cement called bone cement into the vertebral body through the needle. After injection the bone cement hardens, the vertebra is stabilized. In

J. Duncan and G. Gerig (Eds.): MICCAI 2005, LNCS 3750, pp. 105–113, 2005.

this treatment technique, it is one of the most important procedure that the surgeon inserts needle into vertebra precisely. Because the spinal cord and nerves exist through the vertebra, if the surgeon injures nerves by the needle, it will cause critical accidents such as a partial paralysis of the patients. The surgeon must insert needles along appropriate trajectory that locates in a narrow space of pedicle of arch of vertebra. Thus, surgeons must have considerably high skill and experiences in order to control the position of needle. When the needle is inserted percutaneously, the surgeon uses X-ray fluoroscopy to confirm the position of needle resulting in continuous exposure of surgeon's hand to X-ray. A new engineering assistance is required to improve the reliability, accuracy, and safety of this procedure.

In order to improve the above-mentioned subject, we have developed a needle insertion robot for PVP (Figure 2)[1]. Cleary et al. developed needle insertion robot for nerve and facet blocks under X-ray fluoroscopy[2]. Compared with robot for nerve and facet blocks, the robot for PVP must generate larger insertion force to make the needle penetrate cortical bone of vertbra. On the other hand, the size of the robot must be compact. In this report, design of the developed needle insertion robot for percutaneous vertebroplasty, its experimental evaluation on the basic performance of the system and needle insertion accuracy are presented. The positioning accuracy of the robot itself was evaluated and the safety mechanism in case of excessive applied force was also tested. Finally, accuracy of needle insertion of the robot under image guidance was evaluated using a vertebra model.

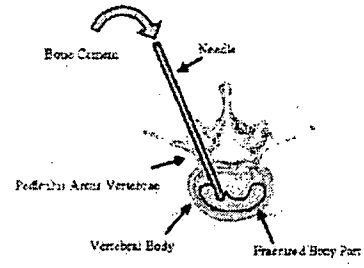

Fig. 1. Percutaneous Vertebroplasty

2 Materials and Methods

Design of the Needle Insertion Robot

The developed robot has the following features:

1. The robot is rigid enough to generate required needle insertion force.
2. The robot is compact so that the robot system (needle positioning mechanism, needle insertion and rotation mechanism) can be inserted in the space between C-arm and the patient on the operating table. We have also developed an X-ray lucent operating table made of carbon reinforced fiber materials (Mizuho Ltd., Japan).
3. The needle holding part of the robot is X-ray lucent so that the needle insertion process can be monitored by fluoroscopy (Figure 3).
4. The position and orientation of the needle can be adjusted with five degrees of freedom in three-dimensional space.

5. The robot system is controlled by the surgical navigation system where the appropriate needle trajectory is planned based on pre-operative three dimensional CT images.
6. The safety mechanism that avoid injury of the patient by the needle when excessive force is applied to the needle due to malfunction of the system.

The needle insertion robot is shown in Figure 2. The robot consists of three parts: 1) Rough positioning mechanism, 2) Accurate positioning mechanism, 3) Puncture mechanism. The rough positioning mechanism does not have any actuator. It has only electro-magnetic brake to fix two joints. (X, and Y in Figure 4). It positions the accurate positioning mechanism and puncture mechanism in two-dimensional plane parallel to the operation bed surface. One actuated translational positioning mechanism is used to position the mechanism in z direction shown in Figure 4.

The accurate positioning mechanism has four degrees of freedom for determination of orientation and position of the puncture mechanism: two DOF for to perpendicular translational motions (± 10 mm in s[1] and s[2] direction shown in Figure 4) and two DOF for rotating motions around two axis intersecting with each other at right angle (± 30 degrees in α and ± 5 degrees in β shown in

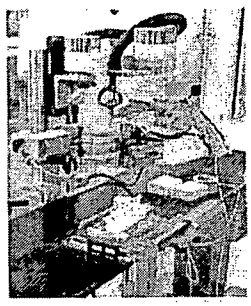

Fig. 2. Developed Needle Insertion Robot

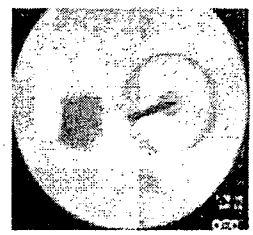

Fig. 3. C-arm X-ray image of the robot which has radiolucent

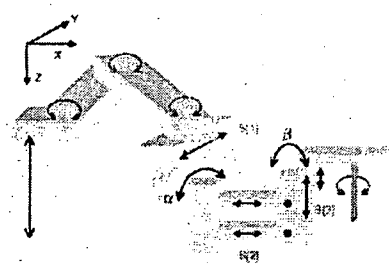

Fig. 4. Robot Mechanism

Figure 4). R-guide was used to realize the rotation for α axis, and remote center of motion mechanism consisting of two linear actuation mechanism was used to reduce the thickness of the mechanism[3].

The puncture mechanism inserts the needle into the patients (shown as s[3] in Figure 4) and rotates the needle in reciprocal manner with amplitude of 120 degrees. The stroke and resolution of the needle insertion mechanism are 110 mm and ± 0.2 mm respectively (Figure 4). The holder is a plastic disk fixed to cylindrical part made of stainless steel that is rotated by a DC motor. Inner diameter of the cylinder is 52 mm. We can observe the position of needle by intra operative X-ray fluoroscopy through the cylinder. Surgeon can monitor the position of the tip of the needle during needle insertion process. It also has a force/torque sensor to measure the force applied on the robot during needle insertion. It is reported that the axial force during needle insertion to human vertebra preserved under formalin fixation. And it is reported that the forces did not exceed 25 N when feed rate of the needle was 0.05-0.5 mm/s. We designed the needle insertion mechanism to generate up to 60 N of axial force.

This robot has safety mechanism, called "Mechanical Fuse" (Figure 5). The needle was fixed on the disk plate. The holder grasps the disk with four contacting parts supported by springs as shown in Figure 6. When unexpected excessive force is applied to a needle, the disk comes off from the holder to avoid possible damage to the patient.

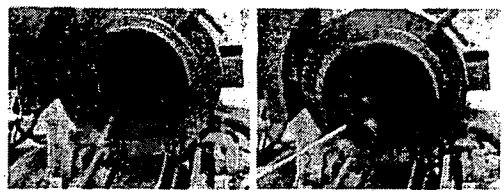

Fig. 5. Left: Normal setting, Right: Situation of Needle comes off by Mechanical Fuse

The entire mechanism was designed to be fixed to the operating table. The size of the entire mechanism was 350 mm × D 400 mm × H270 mm, and its weight was 15 kg. It can be inserted in the space between C-arm of the patient on the operating table as shown in Figure 7.

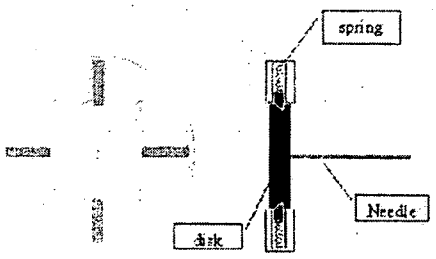

Fig. 6. Mechanism of the Mechanical Fuse

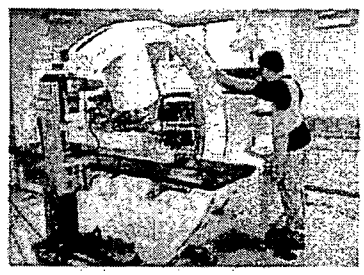

Fig. 7. The robot can be installed between a patient and C-Arm X-Ray Equipment

Description of Control System

Next, control system is shown in Figure 8. The system consists of the following three devices: 1) Needle Insertion Robot, 2) Navigation System([4]), 3) Optical Position Sensor (Optotrak, NDI, Canada). The robot is connected the navigation system by LAN cable (TCP/IP). And the navigation system is connected with an optical Position Sensor by serial cable (RS232C). The navigation system sends the position and orientation data to the robot. The robot drives the target position and orientation using this data by software.

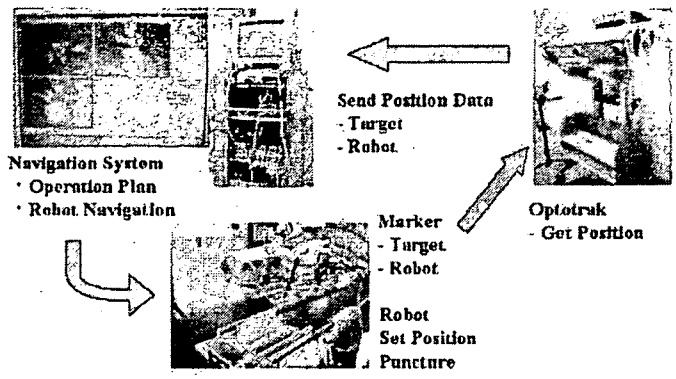

Fig. 8. Total System

Evaluation of Needle Positioning Accuracy

In this study, three experiments were conducted. First experiment is accuracy evaluation of the robot positioning ability. Target values in robot coordinate system were input to the robot and errors between target values and real values which were measured with a position sensor (Polaris, NDI, Canada) placed at the needle insertion mechanism. The errors were evaluated for various points and orientations in the range of motion of the robot.

Second experiment was evaluation of the Mechanical Fuse. The needle was hold by a material-testing instrument with force sensor. The force was applied along the needle and from the direction perpendicular to the needle. The force applied to the needle when the disk came off from the holder was recorded.

Third experiment is evaluation of needle insertion accuracy as a entire system including positioning errors due to needle insertion robot, surgical navigation system, and optical position sensor using a vertebra model (Sawbones, Pacific Research Laboratories, USA). (Figure 9). Three dimensional computer model of the vertebra model was obtained based on its

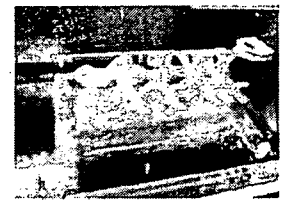

Fig. 9. Polyurethane Vertebra Phantom

CT data. The surface registration was used for surgical navigation [5,6,7,8]. The total errors between target values and determinate needle positions were measured by comparing the planned positions of the needle insertion mechanism and measured position data obtained by the optical position sensor. CT data after the needle insertion was also obtained to identify the difference between the actual needle trajectory and needle insertion plan for one case of the experiments.

The operation with this robot has three stages. At first stage, rough position is set manually. Second, accurate position is set automatically by interaction with the navigation system. Third, needle is inserted to a vertebra.

3 Results

Accuracy Evaluation of the Robot Positioning

Accuracy evaluation is performed on each axis. Result is shown in Table 1. All axes are satisfied requested specifications. However, errors of axis X and Z are somewhat large.

Next, target values in a robot coordinate system are inputted the robot. Result is shown in Table 2. In this case, all axes are satisfied requested specifications, too.

Evaluation of the Mechanical Fuse

Force along the insertion direction larger than 50 N made the disk came off the holder. Needle holding disk came off when force larger than 3 N was applied at the tip of the needle perpendicular to the needle direction. To simulate the possible situation in clinical setting, position of the vertebra model after initial needle insertion was shifted purposely by manual. The needle came off by mechanical fuse successfully. When a vertebra model is moved suddenly, the needle came off from the robot, too.

Evaluation of Puncture in a Vertebra Model

The target value is set by the navigation system with CT image of pre-operation. The position and orientation errors before and after contacting the model were shown in Table 3. The contact of the needle was detected by the force sensor signals from the system.

X-ray images of one vertebra model used in the experiments were obtained by CT to identify the position of holes created by the needle. The position and trajectory of the needle insertion was evaluated as the center of the respected

Table 1. Accuracy evaluation result of each axis (n=)

X (n=15)	Y (n=15)	Z (n=12)	α (n=36)	β (n=27)
0.54 mm	0.09 mm	0.80 mm	0.25 deg	0.41 deg

Table 2. Accuracy evaluation result of multiple axes

	Ave.	SD	Max. Err.
X[mm] (n=675)	-0.437	0.325	-1.197
Y[mm] (n=900)	-0.158	0.197	-0.675
Z[mm] (n=1428)	-0.540	0.361	-1.476
α[deg] (n=2448)	0.122	0.0448	0.230
β[deg] (n=279)	0.138	0.0661	0.364

Table 3. Result of Puncture Experiment

		Average Error ± SD	Maximum Error	Minimum Error
Pre-Puncture (n=10)	Position [mm]	0.80 ± 0.29	1.13	0.31
	Orientation [deg]	0.06 ± 0.08	0.21	0.00
Contact (n=8)	Position [mm]	0.81 ± 0.40	1.51	0.41
	Orientation [deg]	0.20 ± 0.26	0.80	0.03

volume due to needle insertion. The difference between the planned position and the entry point of the needle at the surface was 0.21 mm and the orientation error was 0.9 deg.

4 Discussion

The developed robot is compact enough to be set in the space between C-arm and operating table, while being able to generate required force for needle insertion to vertebra. It can insert 10 G needle into porcine vertebra sample with surrounding tissue and skin (data not shown.) Thus, it can generate enough force for PVP.

In accuracy evaluation, the robot is satisfied requested specifications (error less than 1 mm). The reason that errors of axis X and Z are somewhat large is mechanism of X-axis for small size. We used a remote center of motion mechanism consisting of two linear actuation mechanisms to reduce the thickness of the mechanism placed in the space between the C-arm of the fluoroscopy and operating table. This deteriorates positioning accuracy of the robot. However, since required positioning accuracy was satisfied as a whole. The system has enough positioning accuracy for PVP.

The Mechanical Fuse functioned as designed. For further validation of the mechanical fuse, experiments simulating possible disturbances observed in actual clinical situations to confirm the safety of the system. In addition to the mechanical safety measures, we have to develop the software to stop the system when the abnormal needle force is detected in the embedded force sensors in the system.

In total system error evaluation experiments, average of error is satisfied requested specifications (position error less than 1 mm and orientation error less than 1 deg). However, there was a case of the error exceeding required

specification. We have to investigate the possible causes of errors to reduce the total positioning accuracy. Another possible factor not evaluated in the present study is the slip of the needle tip at the contact to the cortical bone. When the surface of the vertebra is inclined, the needle may slip from the appropriate insertion position. Thus the appropriate needle insertion plan must be designed to reduce the possibility of needle slip based on the geometrical information of the vertebra. Although the system can be inserted into the space between the C-arm and patient on the operating table, the system must be further miniaturized for ease of operation for easier setting and operation. We will analyze the cause of errors and optimize the mechanical design.

5 Conclusion

We have developed a needle insertion robot for Percutaneous Vertebroplasty. Its experimental evaluation on the basic performance of the system and needle insertion accuracy is presented. This robot can puncture with accurate and an operator does not need to be exposed to X-ray. The mechanism of the robot is compact in size (350 mm × D 400 mm × H270 mm, weight: 15 kg) so that the robot system can be inserted in the space between C-arm of the patient on the operating table. The position and orientation of the needle can be adjusted with five degrees of freedom in three-dimensional space. The robot system is controlled by the surgical navigation system where the appropriate needle trajectory is planned based on pre-operative three-dimensional CT images. The needle holding part of the robot is X-ray lucent so that the needle insertion process can be monitored by fluoroscopy. The position of the needle during insertion process can be continuously monitored. In vitro evaluation of the system showed that average positioning and orientation errors were less than 1.0 mm and 1.0 degree respectively. Experimental results showed that the safety mechanism called mechanical fuse released the needle holding disk properly when excessive force was applied to the needle. These experimental results demonstrated that the developed system has the satisfactory basic performance as needle insertion robot for PVP.

Acknowledgement. This study was partly supported by "Research for the Future Program JSPS-RFTF 99I00904"

References

1. Matsumiya, K.: Proc. miccai 2003. Medical Image Computing and Computer-Assisted Intervention (2003) 271–278
2. Cleary, K., Stoianovici, D., Patriciu, A., Mazilu, D., Lindisch, D., Watson, V.: Robotically assisted nerve and facet blocks. Academic Radiology (2002) 821–825
3. Kim, D., Kobayashi, E., Dohi, T., Sakuma, I.: A new, compact mr-compatible surgical manipulator for minimally invasive liver surgery. Lecture Notes in Computer Science **2488** (2002) 99–106

4. Nakajima, Y., Yamamoto, H., Sato, Y., Sugano, N., Momoi, Y., Sasama, T., Koyama, T., Tamura, Y., Yonenobu, K., Sakuma, I., Yoshikawa, H., Ochi, T., Tamura, S.: Available range analysis of laser guidance system and its application to monolithic integration with optical tracker. CARS 2004, Chicago, USA (2004-06)
5. Besl, P.J., Mckay, N.D.: A method for registration of 3-d shapes. IEEE Trans. Pattern Anal. Machin. Intell. 14 (1992) 239–256
6. Simon, D., Hebert, M., Kanade, T.: Techniques for fast and accurate intrasurgical registration. The Journal of Image Guided Surgery 1 (1995) 17–29
7. C.R.Maurer, J.Maciunas, J.M.Fitzpatrick: Registration of head ct images to physical space using a weighted combination of points and surfaces. IEEE Trans. Med. Imag. 17 (1998) 753–761
8. R.Bächler, H.Bunke, L.P.Nolte: Restricted surface matching–numerical optimization and technical evaluation. Computer Aided Surgery 6 (2001) 143–152

Proceedings of the 2005 IEEE
International Conference on Mechatronics
July 10-12, 2005, Taipei, Taiwan

Development of a Computer-Integrated Femoral Head Fracture Reduction System

Mamoru MITSUISHI[1], Naohiko SUGITA[1], Shin'ichi WARISAWA[1], Tatsuya ISHIZUKA[1], Touji NAKAZAWA[2], Nobuhiko SUGANO[3], Kazuo YONENOBU[4], and Ichiro SAKUMA[5]

[1] Department of Engineering Synthesis, School of Engineering, The University of Tokyo, Japan, e-mail: mamoru@nml.t.u-tokyo.ac.jp
[2] THK Co. Ltd., Japan, [3] Graduate School of Medicine, Osaka University, Japan, [4] Osaka Minami National Hospital, Japan
[5] School of Frontier Sciences, The University of Tokyo, Japan

Abstract— The exertion and radiation exposure of a doctor both increase with the number of femur fracture patients treated. The authors have developed a robotic system to assist in the operation, lessen these problems, and improve the efficacy of repair. The robot has 6 degrees of freedom, with a 6-axis force sensor installed to enable a power assist capability for the surgeon and to measure the force applied to the patient's femur. The following three operation modes are provided: JOG mode using a teaching pendant, a power assisted mode and an automatic operation mode. Experiments were successfully performed to evaluate the capabilities of the developed system. The basic data needed to apply the system in clinical use were obtained.

I. Introduction

The prevalence of femur head fracture has been increasing in orthopedic practices recently. It is expected that the number will be increased further in the coming aged society. For femur and tibia fracture therapy, it is possible to reduce the duration of hospital stay, prevent complications, maintain self-support, and reduce the treatment cost if the fractured part of the inferior branch can be fixed securely and with minimal invasiveness using a metal implant. However, the attachment force is not always high enough if the fracture reduction is incomplete. Therefore, three-dimensional, accurate fracture reduction is required and the development of an accurate, image-guided, robotic system for performing bone fracture reduction operations with minimal medical staff is essential.

The conventional reduction procedure is as follows: (1) separation of a piece of bone by pulling the inferior branch (leg), (2) reduction motion by pulling and rotation of an inferior branch, and (3) intra-operative confirmation by X-ray. The conventional procedure, however, has the following problems: (1) The force that must be exerted by the surgeons is large while pulling the inferior branch. (2) Surgeons, medical staff and patients are exposed to radiation during the operation, (3) Reduction accuracy depends on the ability of the surgeon. Therefore, researches concerning accurate navigation in bone fraction reduction systems are crucial [1][2].

The authors have developed a medical robot system to assist in femoral head fraction reduction which solves the problems mentioned above. The developed system was evaluated through experiments. Furthermore, basic data were obtained to apply the robot in a clinical test.

II. Related Work

The progress of applied computer technology in engineering, and in medicine in particular, is remarkable. Starting from various kinds of diagnosis system, computer assisted navigation system is becoming popular, in particular, in orthopedic surgery.

As an example of computer assisted surgery, a system to support the determination of bone cutting and an artificial joint setting position and attitude was developed. Robotic systems to cut bone following the preoperatively planned data have been developed [3][4][5]. ROBODOC [6], CASPER [7], ACROBOT [5] are representative examples of robot-assisted orthopedic systems for total knee arthroplasty. Robot-assisted artificial joint replacement has been executed in several thousand procedures since 1992.

Comparative studies of robot-assisted and traditional surgery are presented in [8], [9] and [10]. Hoal, et al. have performed more than 50 hip joint replacement operations using ROBODOC. The robot-assisted surgery was better than the traditional one in both machining accuracy of bone resection and recovery time of the patient from surgery [8].

In areas other than bone surgery, the Intuitive Surgical da Vinci and ZEUS are well known as endoscopic surgical systems. The former was developed by Salisbury and used a wire-driven type of minimally invasive surgery system. It has seven degrees of freedom on one hand and it is possible to change the forceps part, depending on the task. The forceps have a bending degree of freedom and the force applied on the tip can be fed back to the master manipulator. However, it is impossible to feel the force during manipulation while operating on soft tissue because of the large reduction ratio. ZEUSs are used by arranging them beside the operating table. A tele-surgery experiment was performed between United States and France in 2001. The system obtained approval from the FDA for a remote bilateral operation system named SOCRATES, which provided an environment for surgical guidance by sharing video and audio feeds among remote doctors, connecting the operating room and their offices.

As an example of a bone fracture reduction system, a navigation system to guide bone to the appropriate position using the intra-operative X-ray image has been developed [1][2].

0-7803-8998-0/05/$20.00 ©2005 IEEE

In this paper, the authors have developed a bone fracture reduction assisting system, which consists of a navigation system and a robot system which performs the reduction motion. Moreover, experimental evaluation results and basic biomechanical data for application in clinical use are presented.

III. System Construction

Figure 1 shows an overview of the developed system and Figure 2 shows a schematic diagram of the system. The system consists of a navigation system, a robotic system to realize the reduction motion, an intra-operative X-ray system, and an operation table, the motion of which can synchronize with the bone fraction reduction robot. They are connected to each other through a computer network. The fracture reduction procedure is as follows: (1) The optimum reduction path is calculated pre-operatively using the CT and X-ray images at the navigation system. (2) The calculated path is sent to the reduction robot. (3) The reduction motion is performed by the robot.

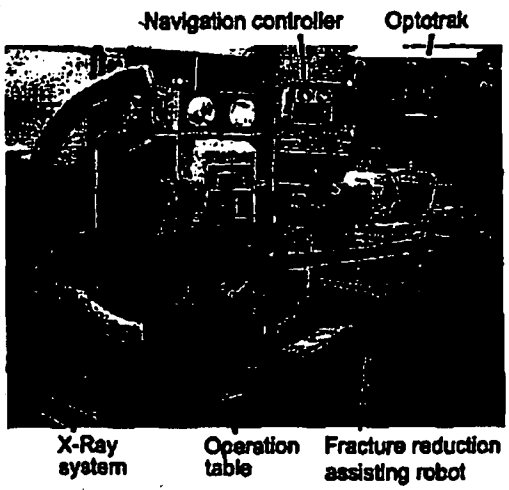

Fig.1 System overview

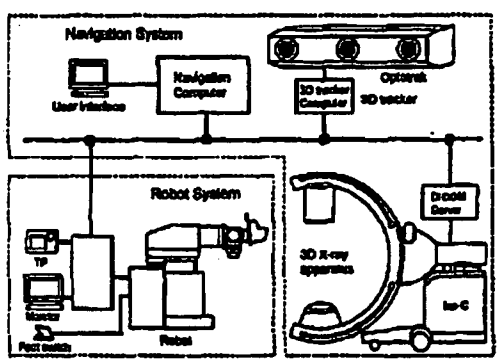

Fig.2 Schematic diagram of the system

IV. Overview of the Navigation System

The system plans the trajectory, including position and posture, of the fractured part from the dislocated position to the reduced one. A navigation system which performs image guided reduction was developed. To obtain the 3 dimensional image, the 3D image can either be obtained intra-operatively or preoperatively using CT. Obtaining the 3D image intra-operatively has the advantage considering cost and time. However, the planning must be performed in the operation room. Therefore, in the developed system, the 3D image has been obtained using CT. The following three strategies can be listed for image guided bone fracture reduction: (1) The opposite side of the inferior branch is considered as a mold. After fitting the proximal part of the bone piece to the mold, the distal part is set to the mold. (2) Matching is executed using the cross sectional information of the broken part. (3) The ante-version angle of the femur head and neck-shaft angle is planned to be the average value. Method (2) is used when the opposite side inferior branch has an abnormality or when an implant has already been applied. Method (3) is used when the information of the opposite side inferior branch cannot be used. The method is also used when the broken cross section is crushed.

V. Fracture Reduction Assisting Robot

A. Required functions

The following functions are required for a femoral head fracture reduction robot.

1) Pulling and rotation function

The distal part of the inferior branch can be fixed by the robot. The pushing/pulling and the rotational motions can be generated in 3 translational and 3 rotational directions, respectively.

2) Safety

(a) Fail-safe mechanism: Large displacement occurs when excessive force is applied to the bone and the fail-safe mechanism limits the force. Fail-safe mechanisms are installed in the pulling and the rotational direction around the femur and tibia bone axes.

(b) Emergency stop function: The system stops moving and maintains the current position when the emergency stop bottom is pushed.

3) Suitability for the operating table located in the operation room

(a) The robot can move in two directions in a plane toward the operation table. The approach posture can be changed freely.

(b) The robot can be connected with the existing operation table. Attaching and detaching operations should be easy.

(c) The same position can be maintained by a lift after the determination of a fracture reduction robot position in the operating room.

(d) The motion of the robot must be synchronized with that of an operation table while moving up and down to maintain the relative position between the body and inferior branches.

4) The following operating modes were prepared: JOG mode, power assisted mode, and an automatic mode.

(a) JOG mode: motion for each axis or complicated movement is possible with a teaching pendant.

(b) Power assisted mode: When limited power is applied to the fracture reduction robot, the power is amplified according to the desired level. Such a function allows the operation for an inferior branch to be executed more easily.

(c) Automatic mode: The motion command is sent from the higher navigation system.

B. Overview of the robot

To realized the required functions mentioned above, the authors have developed a robot with six degrees of freedom yielding three rotational and three translational motions, as shown in Figure 3 and Figure 4. Linear guides were orthogonally assembled to realize the 3 translational motions. For the rotational axes, the axes of all rotational degrees of freedom intersect at the same point using a hollow motor. By adopting these mechanisms, it is easy to calculate the posture. Table 1 shows the main specifications.

The fracture reduction robot can be attached to an operation table using an arm. It is possible to adjust the arm, depending on the length of lower branch of a patient. Furthermore, it is possible to swing the arm in right and left directions. The robot is set rigidly by a lift after the position of robot is determined.

The lower branch of a patient is fixed by a boot. A 6-axis force sensor is mounted between the boot for inferior branch fixation and the motors for the rotational axes. Using the force sensor, it is possible to measure a load applied on the inferior branch of a patient and to implement power assisted operation. The power assisted mode is effective when the foot pedal is pushed.

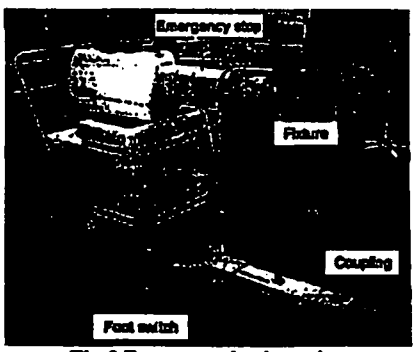

Fig.3 Fracture reduction robot

Table 1 Specification

Stroke	X: ±150mm Y: -10-300mm Z:-10-300mm A: ±20deg. B: ±25deg. C: ±135deg.
Force sensor	Fx, Fy: 400N, Fz: 800N Mx, My, Mz: 40Nm
Fail-safe mechanism	Y: 280N 100mm, 30mm B: 28Nm ±135deg.

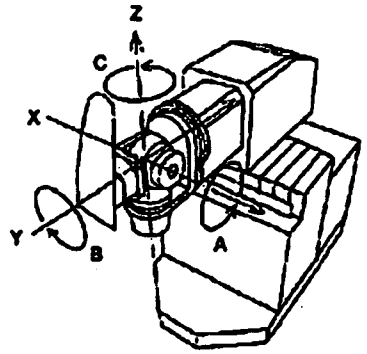

Fig.4 Definition of each axis

Part of the operation table is made of carbon fiber reinforced composites to allow clean 2 dimensional and 3 dimensional images to be obtained by a C-arm during the operation.

C. Fail-safe mechanism

When excessive force is applied on an inferior branch during fracture reduction, both ligament and muscle may be damaged and a new bone fracture may be caused. Therefore, it is necessary to prevent any overload on the inferior branch. Because a multi-axis force sensor is mounted on the robot, it seems possible to stop the system by monitoring the overload. However, it is uncertain whether the measured force is reliable during an emergency, since there is a possibility that the multi-axis force sensor has been damaged. Therefore, a hardware fail-safe mechanism has been installed. Functions required for a hardware fail-safe system are as follows: (1) High rigidity should be maintained in normal state. (2) Large displacement occurs when an excessive force is applied to the system as the fail-safe system limits the force. (3) Emergency signal is generated and the system is stopped. (4) When the excessive force is removed, the system returns to its normal state.

To realize these functions, a ball was put in a cone-shaped hole, and it was pushed with a spring from the top (plunger method).

It is possible to adjust the fail-safe load because the spring force is variable.

D. Control system

RT-Linux was adopted as an OS of the reduction system. There are three kinds of tasks for the control system as shown in Fig.5: (1) a robot control task, (2) a socket communication control task, and (3) a teaching pendant control task. The robot control task, which is a real-time task, is executed at 1kHz. The socket communication control task and the teaching pendant task are executed in the user task area. Each task is connected through a FIFO buffer.

As mentioned above, the following control modes were implemented in the fracture reduction system: JOG mode, power assisted mode, and automatic mode. Among these modes, the power assisted mode is outstanding.

In the power assisted mode, the force which is applied to the

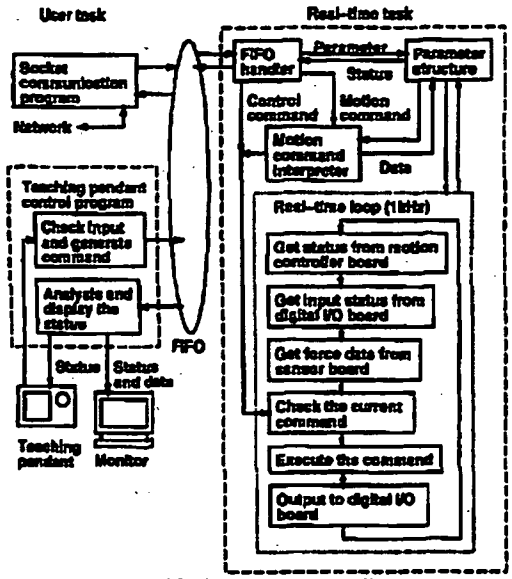

Fig.5 Robot system controller

patient's inferior branch by a surgeon is detected by the multi-axis force sensor. The detected force is used to realize proportional control by moving the inferior branch to an arbitrary position and posture. When the surgeon applies a force to the boot which fixes the inferior branch, the multi-axis force sensor measures the resultant force that the reduction robot applies to the inferior branch and that the surgeon applies to the inferior branch. The force, which a surgeon applies to the inferior branch, is denoted "assist force" in this paper. It is impossible, therefore, to detect only the force which the surgeon applies to the inferior branch. Generally, two force sensors are necessary to detect the force independently. However, in the developed system, a foot switch was prepared. The assist force is considered at the origin when the foot switch is pressed. The variance of the force while pressing the foot switch is considered as an assist force. In the implemented system, the motion of the fracture reduction robot was controlled to make the variance force zero (Fig. 6).

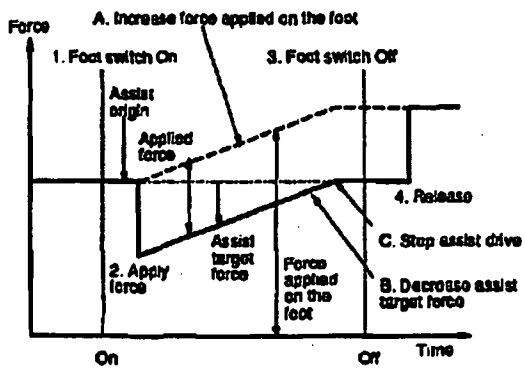

Fig.6 Power assisted mode

The assist force is calculated to be small if the motion of the fracture reduction robot increases the force applied to the patient's inferior branch. Consequently, the motion of the robot is stopped. Therefore, the robot is safe. The motion of the robot is stopped when the increase of the force applied to the inferior branch and the force applied to the boot by the surgeon are equal. Basically, the pulling force is generated by the fracture reduction robot and, therefore, it is possible to reduce the load on the surgeon. When the assist motion is stopped, it is possible to regenerate the motion by pushing the foot switch. The motion of the robot is stopped when the foot switch is released. It is possible to stop the motion of the robot immediately if the surgeon detects an abnormal state.

E. Kinematics of the robot

Figure 7 shows the mechanism of the robot. $\vec{C}$, $\vec{L}$ and E represent a vector whose length does not vary, a vector whose length varies, and a rotational matrix, respectively. The suffixes i, j and k represent the X, Y and Z directions, respectively. The mechanism solution is as follows:

$$E = E^{j\theta_1} E^{i\theta_2} E^{i\theta_3}. \quad (1)$$

The characteristic equation is presented as

$$\vec{P} = \vec{L}_1^j + \vec{L}_2^j + \vec{C}_3^k + \vec{L}_4^j + \vec{C}_5^k + \vec{C}_6^j + E^{j\theta_1}(\vec{C}_7^k + \vec{C}_8^j + E^{k\theta_9}(\vec{C}_9^k + \vec{C}_{10}^i + E^{i\theta_{11}}\vec{C}_{11}^j)). \quad (2)$$

The position and the attitude of the robot can be solved using these equations.

VI. Evaluation of the Developed Functions

A. Fail-safe mechanism

The functioning of the fail-safe mechanism, which releases the overload, was evaluated. The activation threshholds points of the mechanism was set as 280 N, plus or minus 25 Nm, for Y-axis and B-axis. In the experiment, the value of

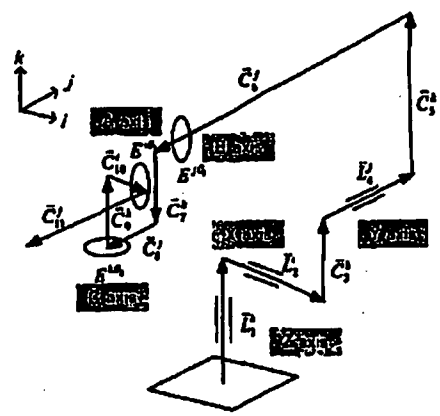

Fig.7 Kinematics of the developed fracture reduction assisting robot

the activation threshold was measured. Figure 8 shows the relationship between the force and the position. It was possible to confirm that the realized activation threshold corresponds well with the desired value.

B. Power assisted function

The power assisted mode was implemented to reduce the load on a surgeon when pulling and rotating the patient's inferior branch using the control strategy mentioned above. The force applied to the boot by the surgeon was measured by a 6-axis force sensor. The motors were controlled depending on the direction and the value of the measured force. The power assisted mode is operative only while the foot pedal is pushed.

It is possible to modify the viscosity of the system by changing the acceleration depending on the detected force. Figures 9 and 10 show the relationship between the applied force and the position along the B-axis. Figures 9 and 10 represent the experimental results for the "soft mode" and "hard mode," respectively. In both figures, the relationship between the position and the force is presented, until the system reaches the appropriate position by repeating the On/Off for the foot switch. The motion distance is accumulated even if the origin of the calculated force is reset to zero using the On and Off of the foot switch. The required time is small in the case of the "soft mode" as shown in Fig. 9. In this case, the motion distance caused by a unit force is large. On the contrary, the motion distance is small in case of "hard mode" as shown in Fig.10.

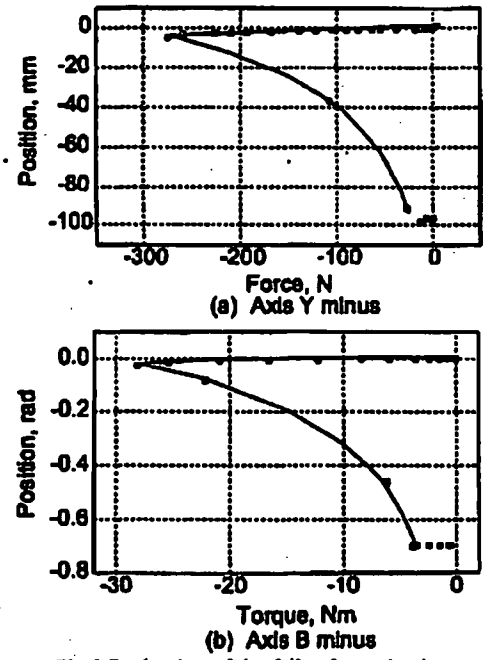

Fig.8 Evaluation of the fail-safe mechanism

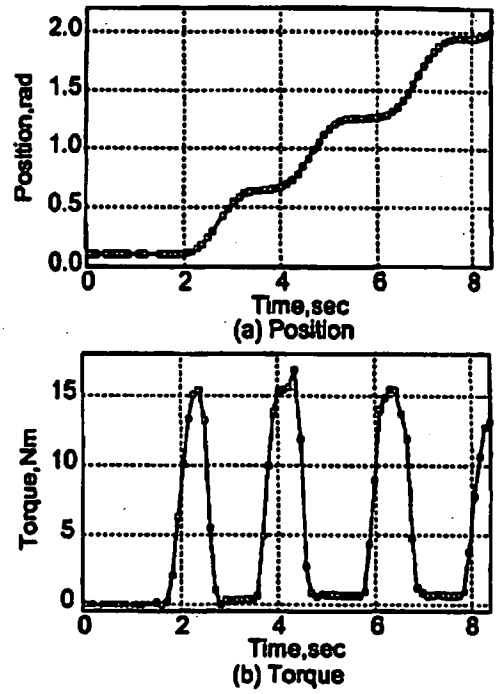

Fig.9 Power assist in soft mode

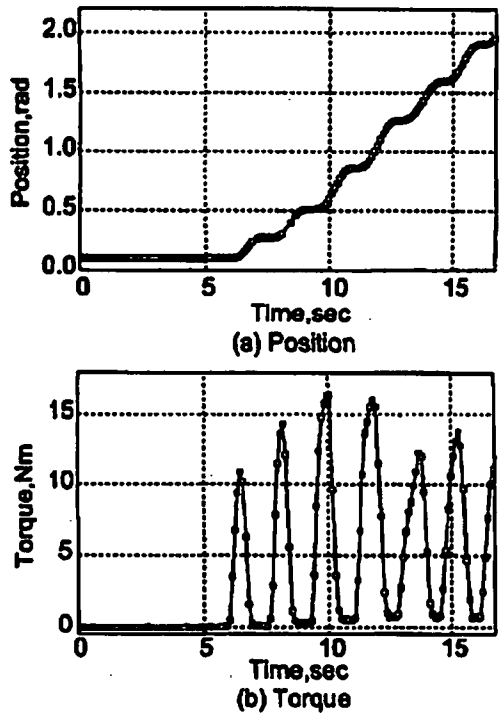

Fig.10 Power assist in hard mode

C. Application to the human body

Basic data were obtained needed to apply the robot to a clinical test. The relationship between the distance and the load was measured. Furthermore, the motion range of the